

We are IntechOpen, the world's leading publisher of Open Access books Built by scientists, for scientists

6,900

Open access books available

186,000

International authors and editors

200M

Downloads

Our authors are among the

154

Countries delivered to

TOP 1%

most cited scientists

12.2%

Contributors from top 500 universities



WEB OF SCIENCE™

Selection of our books indexed in the Book Citation Index
in Web of Science™ Core Collection (BKCI)

Interested in publishing with us?
Contact book.department@intechopen.com

Numbers displayed above are based on latest data collected.
For more information visit www.intechopen.com



Photo-induced Effect in Quantum Paraelectric Materials Studied by Transient Birefringence Measurement

Toshiro Kohmoto and Yuka Koyama
*Graduate School of Science, Kobe University,
 Japan*

1. Introduction

Strontium titanate SrTiO_3 is known as a quantum paraelectric material, and its lattice dynamics and unusual dielectric character have been studied extensively. The cubic (O_h) structure above the structural phase transition temperature ($T_C = 105$ K) changes into the tetragonal (D_{4h}) structure below T_C . At low temperatures, dielectric constant increases up to about 3×10^4 , where the paraelectric phase is stabilized by quantum fluctuations even below the classical Curie temperature 37 K (Muller & Burkard, 1979).

Photo-induced effect in dielectric materials is an attractive topic. Some kind of ferroelectric materials such as SbSI (Ueda et al., 1967) and BaTiO_3 (Volk et al., 1973; Godefroy et al., 1976) are known to show photo-induced effects. In this decade, much interest has been paid on the giant enhancement in dielectric constants under ultraviolet (UV) illumination and DC electric field in quantum paraelectrics, strontium titanate SrTiO_3 and potassium tantalate KTaO_3 (Takesada et al., 2003; Hasegawa et al., 2003; Katayama et al., 2003), because weak light illumination gives rise to an intense response in dielectricity.

The two models shown Fig. 1, the ferroelectric cluster model (Takesada et al., 2003; Hasegawa et al., 2003; Katayama et al., 2003) and the conductive-region model (Homes et al., 2001; Katayama et al., 2003), have been proposed to explain the origin of the giant dielectric constants. At present, however, it is still not clear which model is better. In the ferroelectric cluster model, the photo-induced ferroelectric region has a huge dipole moment, where it is expected that a photo-induced polar domain generates spatial lattice distortion. In the conductive-region model, on the other hand, the superposition of insulative and photo-induced conductive regions, which is characterized by the boundaries between the two regions, makes the apparent dielectric constants to be enormous.

Giant dielectric response has been observed in some types of nonferroelectric materials (Homes et al., 2001; Wu et al., 2002; Dwivedi et al., 2010). The enormous increase in dielectric constants is attributed to the formation of barrier layer capacitors and the resultant Maxwell-Wagner polarization or interfacial polarization. This giant dielectric response often occurs in materials with grains surrounded by the insulating grain boundary and is explained by the conductive-region model.

According to the measurement of dielectric constants, a doped crystal $\text{Sr}_{1-x}\text{Ca}_x\text{TiO}_3$ undergoes a ferroelectric transition above the critical Ca concentration $x_c = 0.0018$ (Bednorz

& Muller, 1984; Bianchi et al., 1994). Doped Ca ions are substituted for the Sr ions. The cubic structure above the structural phase transition temperature (T_{C1}) changes into the tetragonal structure below T_{C1} and into the rhombohedral structure below the ferroelectric transition temperature T_{C2} . Off-centered impurity ions, which are assumed in the case of impurity systems such as Li-doped KTiO_3 and Nb-doped KTiO_3 (Vugmeister & Glinchuk, 1990), are supposed also in the case of Ca-doped SrTiO_3 . Their polarized dipole moments show a ferroelectric instability below the ferroelectric transition temperature. In the case of Ca-doped SrTiO_3 , a spontaneous polarization occurs along $[110]$ directions within the c plane, where the tetragonal (D_{4h}) symmetry is lowered to C_{2v} .

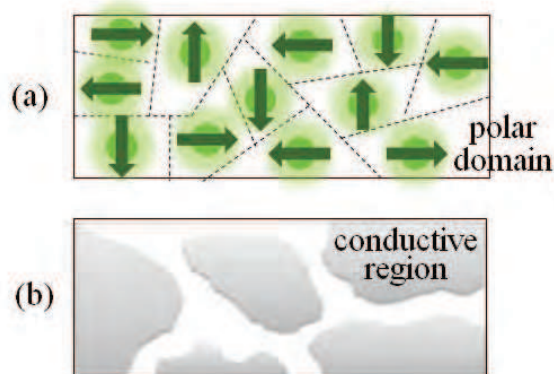


Fig. 1. Schematic pictures of (a) ferroelectric cluster model and (b) conductive-region model.

In Ca-doped SrTiO_3 , a UV illumination causes a shift of the ferroelectric phase transition temperature toward the lower side (Yamada & Tanaka, 2008). The T_{C2} reduction under the UV illumination is considered to be caused by disequilibrium carriers which are captured by traps and screen the polarization field.

In the present study, we performed three types of experiment in pure and Ca-doped SrTiO_3 ; (i) stationary birefringence measurement in UV light and DC electric fields, (ii) transient birefringence measurement in UV light and pulsed electric fields, and (iii) transient absorption and birefringence measurements after the optical pulse excitation using the pump-probe technique. The photo-induced dynamics of the lattice distortion, the dielectric polarization, and the relaxed excited state in SrTiO_3 is studied in comparison with the lattice distortion in the doping-induced ferroelectric phase of Ca-doped SrTiO_3 . We discuss which model explains the experimental results better.

The experiments are performed on single crystals of pure and Ca-doped SrTiO_3 with the Ca concentration of $x = 0.011$. SrTiO_3 was obtained commercially and Ca-doped SrTiO_3 was grown by the floating zone method. The thickness of the samples is 0.2 mm. The structural phase-transition temperature, $T_{C1}=180\text{K}$, of the Ca-doped SrTiO_3 was obtained from the temperature dependence of the birefringence (Koyama et al., 2010), and the ferroelectric phase-transition temperature, $T_{C2} = 28\text{K}$, was determined by the measurement of dielectric constants (Yamada & Tanaka, 2008).

2. Lattice distortion in the UV and DC fields in Ca-doped SrTiO_3

The stationary birefringence is studied to investigate the static properties of the lattice distortion generated by the UV illumination in comparison with that generated by the ferroelectric deformation.

2.1 Birefringence measurement in the UV light and DC electric fields

The schematic diagram of the birefringence measurement in the UV light and DC electric fields is shown in Fig. 2. The change in birefringence is detected as the change in the polarization of a linearly polarized probe light provided by a Nd:YAG laser (532 nm). The source of UV illumination is provided by the second harmonics (380 nm, 3.3 eV) of the output from a mode-locked Ti-sapphire laser, whose energy is larger than the optical band gap of SrTiO_3 (3.2 eV). The intensity of UV illumination is 1.6 mW/mm^2 . Since the repetition rate of the UV pulses is 80 MHz, this UV illumination can be considered to be continuous in the present experiment. The UV beam is illuminated on the gap between two Au electrodes. The electrodes with a gap of 0.8 mm are deposited on a (100) surface of the samples by sputtering. A DC electric field, whose amplitude is 375 V/mm, is applied between the two electrodes. The DC electric field is applied parallel to [100] direction of the crystal.

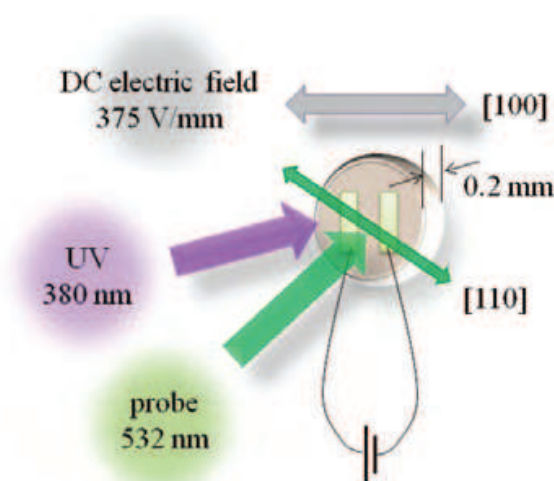


Fig. 2. Schematic diagram of the birefringence measurement in the UV light and DC electric fields.

The change in the polarization of the probe light is detected by a polarimeter. The construction of the polarimeter is shown in Fig. 3. The polarimeter (Kohmoto et al., 2000; Jones, 1976) detects the rotation of polarization plane of a light beam. A linearly-polarized beam is split by a polarized beam splitter (PBS) and incident on the two photodiodes (PD) whose photocurrents are subtracted at a resistor (R). When the polarized beam splitter is mounted at an angle of 45° to the plane of polarization of the light beam, the two photocurrents cancel. If the plane of polarization rotates, the two currents do not cancel and the voltage appears at the resistor.

In the present experiment, the birefringence generated by the lattice deformation is detected as the change in polarization of the probe beam using a quarterwave plate and a polarimeter. The birefringence generated in the sample changes the linear polarization before transmission to an elliptical polarization after transmission. The linearly-polarized probe beam is considered to be a superposition of two circularly-polarized components which have the opposite polarizations and the same intensities. The generated birefringence destroys the intensity balance between the two components. The two circularly-polarized beams are transformed by the quarterwave plate to two linearly-polarized beams whose polarizations are crossed each other, and the unbalance of circular polarization is

transformed to the unbalance of linear polarization or the rotation of polarization plane. This rotation is detected by the polarimeter as the signal of the lattice deformation.

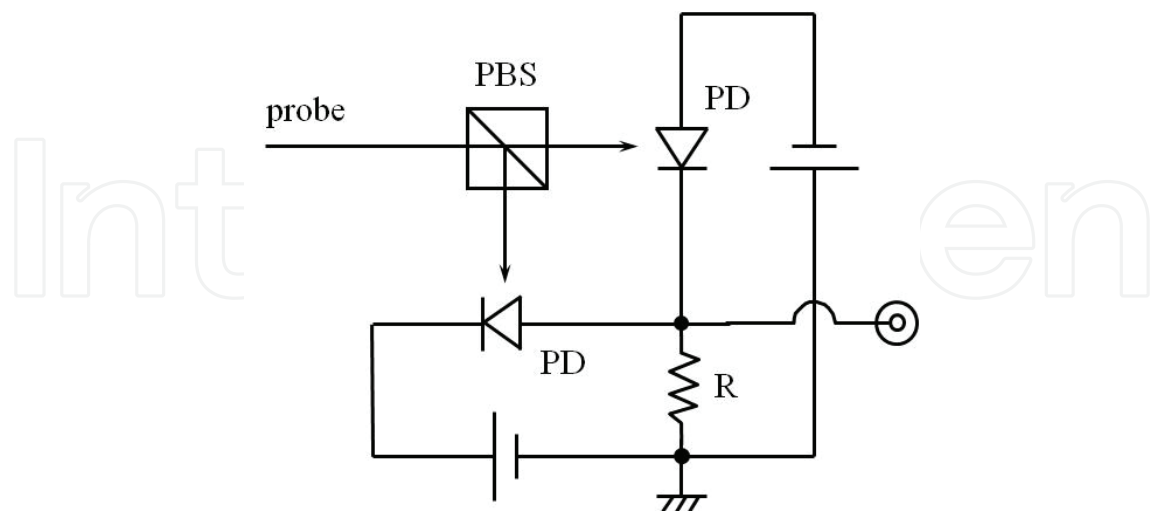


Fig. 3. Construction of the polarimeter.

2.2 UV intensity dependence of the birefringence

The ultraviolet intensity dependence of the change in birefringence in Ca-doped SrTiO_3 is shown in Fig. 4, where the temperature is 6 K and the polarization plane of the probe light is along the $[110]$ and $[100]$ axes, with which the lattice distortion along the $[100]$ and $[110]$ axes are detected, respectively. The birefringence increases nonlinearly as the UV intensity is increased. As is shown in Fig. 4(a), the change in birefringence appears at very weak UV intensity in the polarization plane only along the $[110]$ axis, rises rapidly, and holds almost a constant value above 0.5 mW/mm^2 . Figure 4(b), where the horizontal axis is in a logarithmic scale, indicates that the structural deformation begins at the UV intensity of 10^{-3} mW/mm^2 . The change in birefringence for the probe polarization along the $[110]$ axis is much larger than that along the $[100]$ axis. These facts imply that the UV illumination causes Ca-doped SrTiO_3 to undergo a first-order-like structural deformation and generates a lattice distortion along the $[100]$ axis as a result of the competition between the UV-induced and ferroelectric deformations, and its threshold value is very small.

Figure 5 schematically shows the direction of the local lattice distortion in pure and Ca-doped SrTiO_3 . The observed direction of the lattice distortion in Ca-doped SrTiO_3 generated by the UV illumination is the same as that in the case of pure SrTiO_3 (Nasu, 2003).

2.3 Temperature dependence of the birefringence in the UV and DC fields

We investigated the temperature dependence of the change in birefringence for Ca-doped SrTiO_3 in the combination of two external fields, UV light (UV) and DC electric (DC) fields. The experimental result is shown in Fig. 6 where the polarization plane of the probe light is along the $[110]$ and $[100]$ axes. The sample is in the four types of fields; neither UV nor DC (no field), only DC (DC), only UV (UV), and both UV and DC (UV+DC). The changes in birefringence for the probe polarization along the $[110]$ axis are much larger than those along the $[100]$ axis. This means that the optical anisotropy is generated along the $[100]$ axis. For the probe polarization along the $[110]$ axis without the DC electric field, the change in birefringence for no field is similar to that for UV, as is seen in Fig. 6, while under the DC

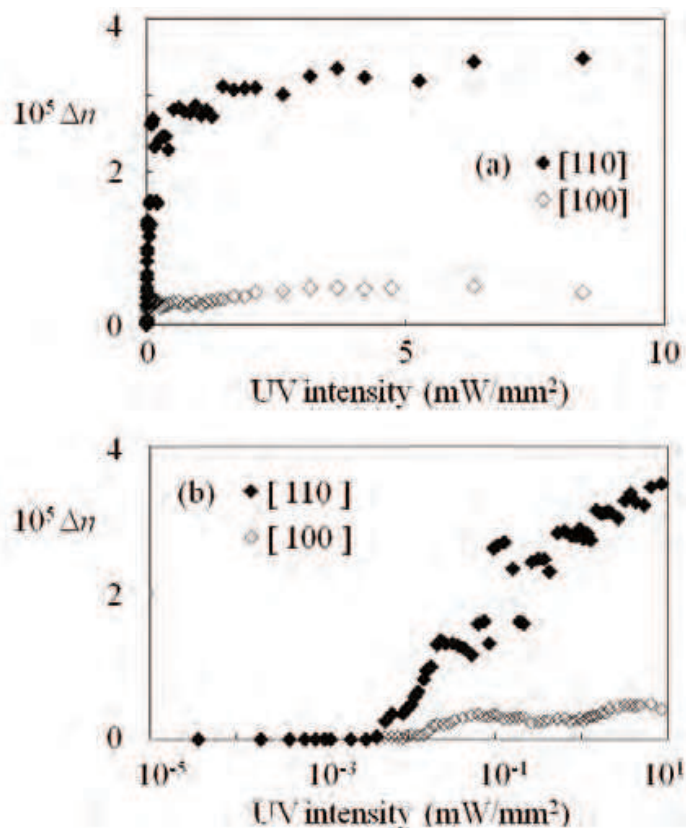


Fig. 4. UV intensity dependence of the change Δn in birefringence in Ca-doped SrTiO_3 at 6 K, where the probe-light polarization is along the $[110]$ and $[100]$ axes. The horizontal axis is (a) in a linear scale and (b) in a logarithmic scale.

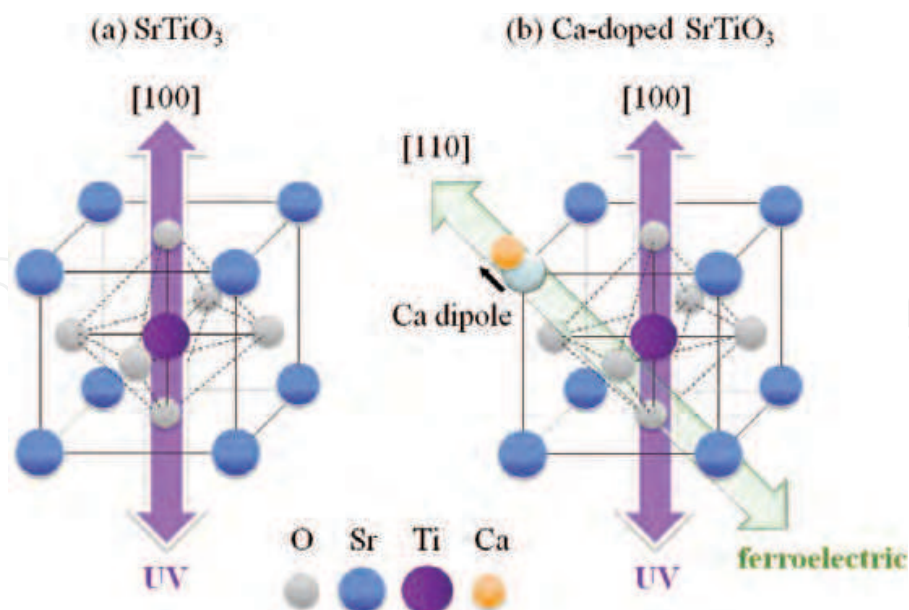


Fig. 5. Direction of the local lattice distortion (a) in SrTiO_3 and (b) in Ca-doped SrTiO_3 . The direction of local lattice distortion generated by the UV illumination is axial along the $[100]$ axis both for pure and Ca-doped SrTiO_3 . The direction of the local lattice distortion in the ferroelectric phase of Ca-doped SrTiO_3 is diagonal along the $[110]$ axis.

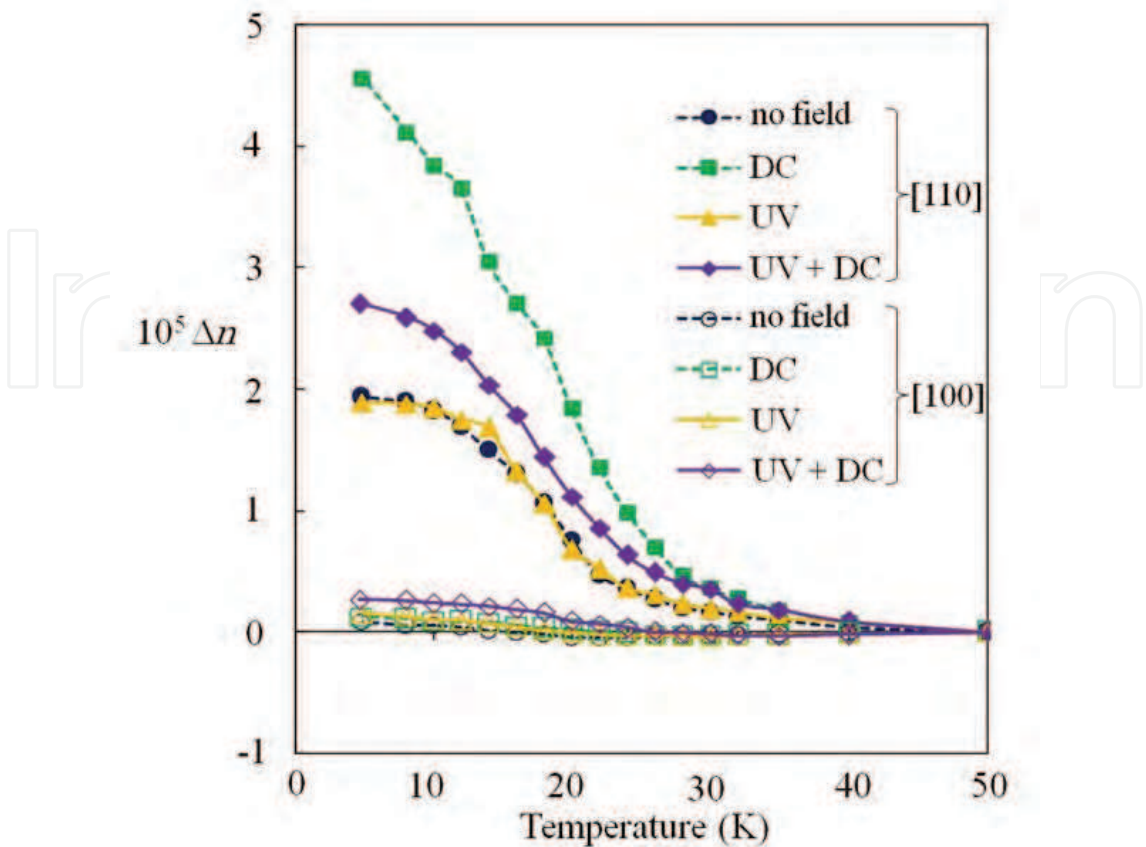


Fig. 6. Temperature dependence of the change in birefringence for Ca-doped SrTiO₃ in the combination of two external fields, UV light (UV) and DC electric (DC) fields, where the polarization plane of the probe light is along the [110] and [100] axes. The sample is in the four types of fields; neither UV nor DC (no field), only DC (DC), only UV (UV), and both UV and DC (UV+DC).

electric field the change for DC is different from that for UV+DC. The difference arises from that of the macroscopic optical anisotropy generated along the [100] axis by the UV illumination.

In the ferroelectric phase of Ca-doped SrTiO₃, the direction of the local lattice distortion is diagonal along the [110] axis (Bednorz & Muller, 1984) as shown in Fig. 5(b). There are six equivalent diagonal sites where the distortion directions are [110], [1-10], [011], [01-1], [101], and [10-1]. In no field, it is expected that the six local sites distribute randomly as shown in Fig. 7(a), and no optical anisotropy is generated. The observed birefringence change Δn_{NO} for no field, however, shows that the optical anisotropy grows along the [100] axis at low temperatures. This may be because that the domain structure due to the structural phase transition violates the equivalency among the six sites.

In the DC electric field along the [100] axis, on the other hand, the six local diagonal sites in the ferroelectric phase are not equivalent as shown in Fig. 7(b). The two diagonal sites, [011] and [01-1] which are perpendicular to the [100] axis, are more unstable in the DC elected field along the [100] axis than the other four diagonal sites, [110], [1-10], [101], and [10-1]. The random distribution of the four diagonal sites generate a macroscopic optical anisotropy along the [100] axis. This explains the observed large increase of the birefringence change Δn_{DC} for the [110] probe and small change for the [100] probe.

As discussed in section 2.2, the lattice distortion generated by the UV illumination is axial along the $[100]$ axis. In no DC electric field, its direction distributes randomly among the three equivalent directions, $[100]$, $[010]$, and $[001]$ as shown in Fig. 7(c), where no macroscopic optical anisotropy is expected. The observed similar behavior between the birefringence changes Δn_{NO} for no field and Δn_{UV} for UV can be explained by the fact that the UV illumination changes the local distortion but does not add any macroscopic optical anisotropy.

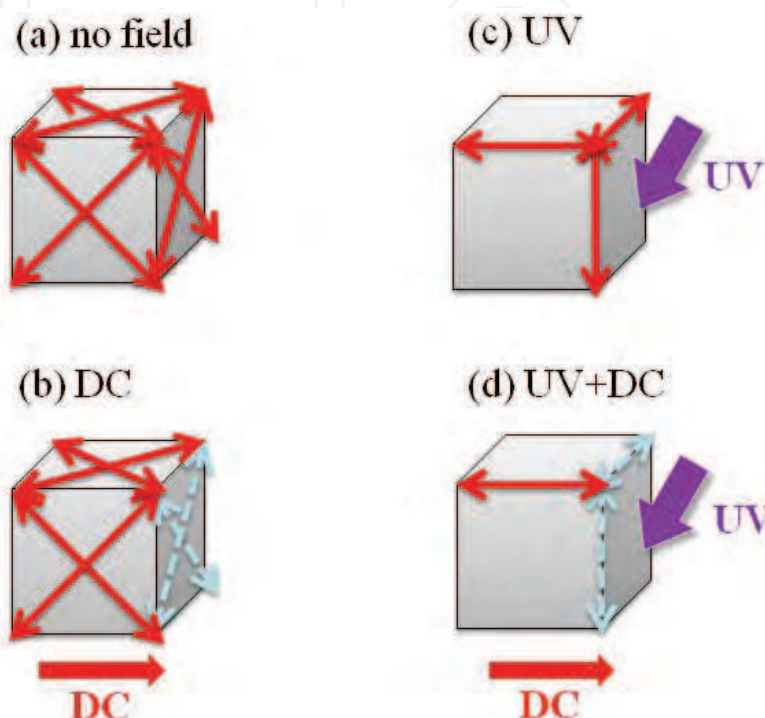


Fig. 7. Directions of the local lattice distortion in the ferroelectric phase of Ca-doped SrTiO_3 . (a) In no field, the six equivalent diagonal sites distribute randomly. (b) In the DC electric field along the $[100]$ axis, the two diagonal sites perpendicular to the $[100]$ axis are more unstable than the other four diagonal sites. (c) The three equivalent axial sites generated by the UV illumination distribute randomly in no DC electric field. (d) In the DC electric field, the two UV-generated axial sites perpendicular to the DC field direction are more unstable than the parallel UV-generated axial site. Macroscopic optical anisotropies are expected to be generated in the DC electric field (b) for DC and (d) for UV+DC, but are not expected (a) for no field and (c) for UV.

In the DC electric field along the $[100]$ axis, the three axial sites generated by the UV illumination are not equivalent as shown in Fig. 7(d). The two axial sites $[010]$ and $[001]$, which are perpendicular to the $[100]$ axis, are more unstable than the other axial site $[100]$. This axial site can also contribute to generate a macroscopic optical anisotropy along the $[100]$ axis. The UV illumination changes some part of the local distortion from the diagonal site along the $[110]$ axis to the axial site along the $[100]$ axis. The UV illumination decreases the birefringence change in the DC electric field; $\Delta n_{\text{UV+DC}} < \Delta n_{\text{DC}}$, as is seen in Fig. 6. This result suggests that the sign of the optical anisotropy generated by the UV illumination is opposite to that by the diagonal distortion in the ferroelectric phase. It should be noted that the optical anisotropy due to the structural deformation generated by the UV illumination is of the same order of magnitude as that generated by the ferroelectric deformation.

3. Lattice distortion in the UV and pulsed electric fields in pure and Ca-doped SrTiO₃

3.1 Transient birefringence measurement in the UV light and pulsed electric fields

The transient birefringence in a pulsed electric field is studied to probe whether or not the lattice distortion generated by the UV illumination is affected by the electric field. In the experiment of transient birefringence, the change in birefringence is monitored by the probe light of 532 nm from the Nd:YAG laser, and its time evolution is obtained from the waveform digitized on an oscilloscope. A pulsed electric field, whose amplitude is 150 V/mm and pulse width is 1.2 ms, is applied between the two Au electrodes.

3.2 Transient birefringence in SrTiO₃

Figure 8(a) shows the change $\Delta n(t)$ in birefringence in pure SrTiO₃ after the application of the electric-field pulse at $t = 0$ between 4.5 K and 50 K, where the UV illumination is off and the polarization plane of the probe light is along the [110] axis. The signal of the birefringence change rises rapidly at the start of the electric-field pulse and holds a constant value during the pulse. As the temperature is decreased, the birefringence change induced by the electric-field pulse is increased. This means that the polarization, which is related to the dielectric constants, is increased at lower temperatures.

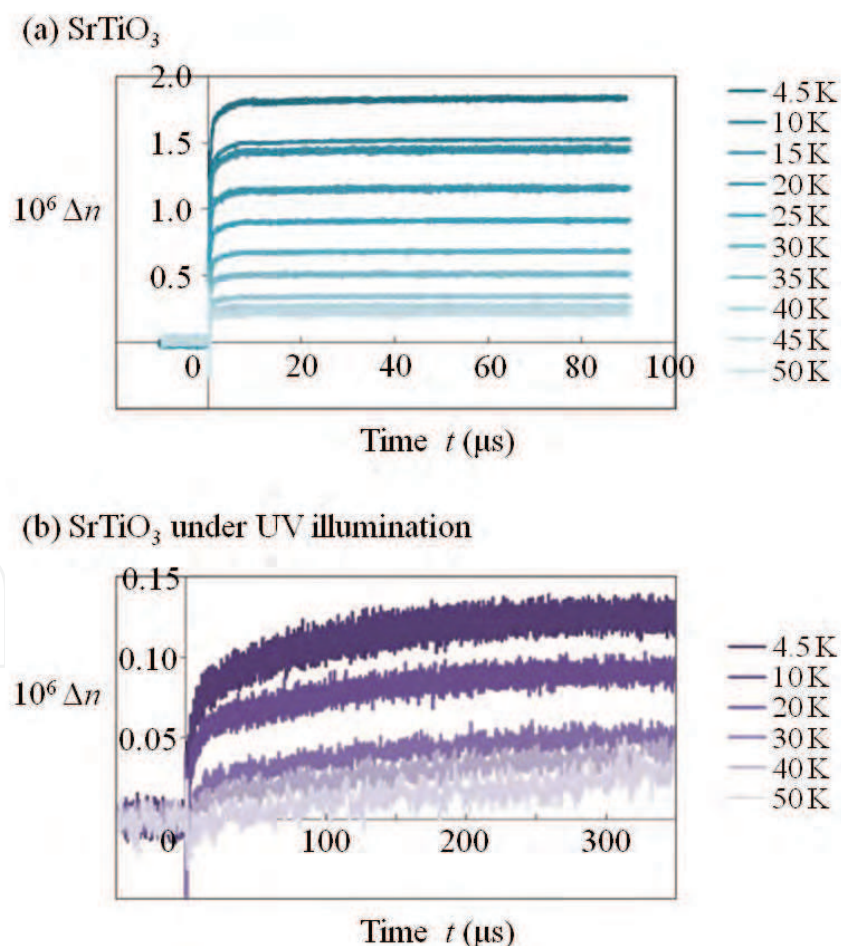


Fig. 8. Temperature dependence of the transient birefringence signal $\Delta n(t)$ in SrTiO₃ in a pulsed electric field under the (a) dark and (b) UV illumination. The polarization plane of the probe light is along the [110] axis. The electric field of 150 V/mm is turned on at $t = 0$.

Figure 8(b) shows the change in birefringence in SrTiO_3 under the UV illumination. The dielectric response of relaxation type is observed at all temperatures. As the temperature is decreased, the relaxation rate becomes increased.

3.3 Transient birefringence in Ca-doped SrTiO_3

The change $\Delta n(t)$ in birefringence in Ca-doped SrTiO_3 is shown in Fig. 9(a), where some oscillating components appear. As the temperature is decreased, the amplitudes of these oscillating components are increased. These oscillations are considered to be caused by the doped Ca ions because they are not observed in pure SrTiO_3 but only in Ca-doped SrTiO_3 . The change in birefringence induced by the electric-field pulse is increased as the temperature is decreased, as well as in SrTiO_3 , which means that the dielectric polarization is increased at low temperatures. Figure 9(b) shows the change in birefringence in Ca-doped SrTiO_3 under the UV illumination. In Ca-doped SrTiO_3 , the dielectric response of relaxation type appears only above the ferroelectric phase transition temperature T_{c2} , and the oscillating components also disappear above T_{c2} .

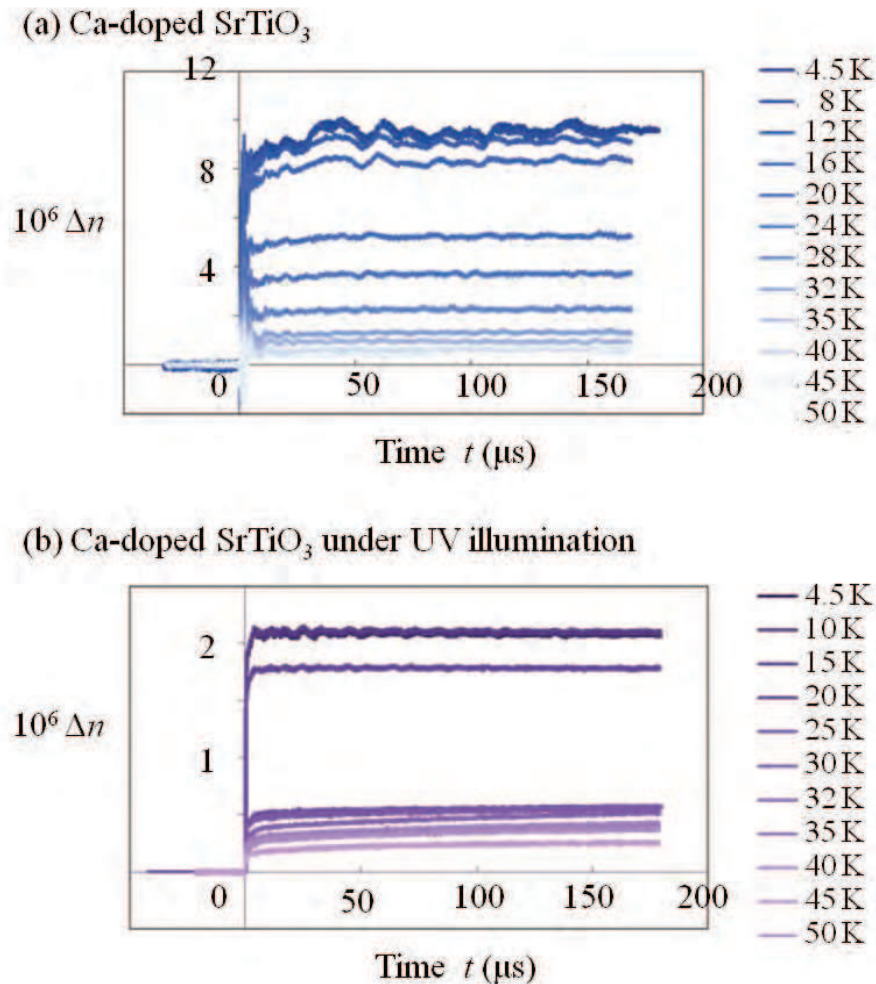


Fig. 9. Temperature dependence of the transient birefringence signal $\Delta n(t)$ in Ca- SrTiO_3 in a pulsed electric field under the (a) dark and (b) UV illumination. The polarization plane of the probe light is along the $[110]$ axis. The electric field of 150 V/mm is turned on at $t = 0$.

3.4 Temperature dependence of the transient birefringence amplitude

The temperature dependences of the transient birefringence amplitude Δn_s for pure and Ca-doped SrTiO₃ are shown in Fig. 10, where Δn_s is obtained from the value of $\Delta n(t)$ at large enough time t in Figs. 8 and 9.

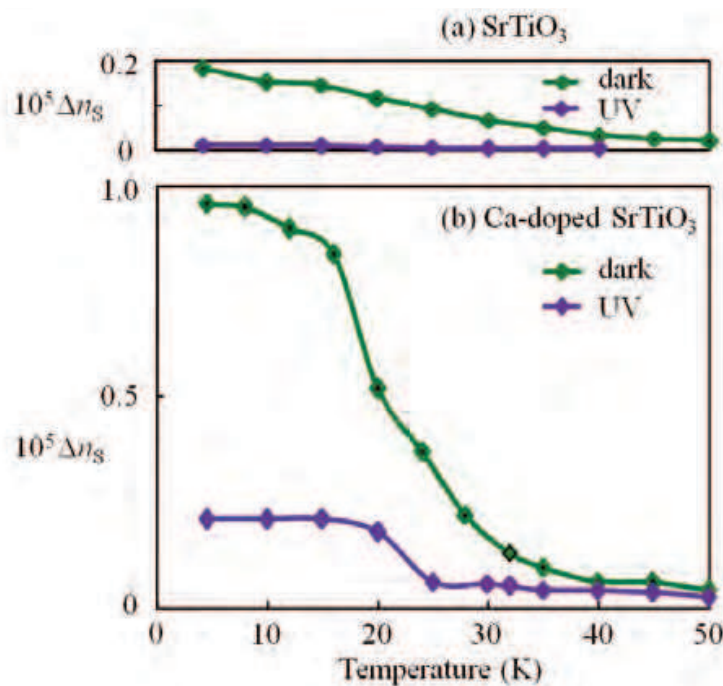


Fig. 10. Temperature dependence of the transient birefringence amplitude Δn_s induced by the electric-field pulse under the dark and UV illumination (a) in SrTiO₃ and (b) in Ca-doped SrTiO₃.

For both samples, it is clear that the transient birefringence amplitude for the probe polarization along the [110] axis is reduced by the UV illumination, which indicates that the lattice deformation is reduced by the UV illumination and that the lattice distortion generated by the UV illumination is not affected by the electric field. This result is not consistent with the ferroelectric cluster model, where a large change in birefringence is expected in the pulsed electric field.

In Ca-doped SrTiO₃, judging from the rising temperature of the transient birefringence amplitude, the ferroelectric phase transition temperature is shifted toward the lower temperature side under the UV illumination. This is consistent with the dielectric measurement (Yamada & Tanaka, 2008) and the coherent phonon experiment (Koyama et al., 2010). The doped Ca ions behave as permanent dipoles, and ferroelectric clusters are formed around the Ca dipoles with the high polarizability of the host crystal. The ferroelectric transition is caused by the ordering of the randomly distributed Ca dipoles. The ordering is prevented by the photo-excited carriers generated by the UV illumination.

4. Dynamics of the relaxed excited state after the optical pulse excitation in SrTiO₃

Figure 11 illustrates the electronic states in SrTiO₃. The UV illumination, whose photon energy is larger than the band-gap energy of SrTiO₃ (3.2 eV), excites the electrons from the ground

state to the excited state. The excited electrons are self-trapped in the relaxed excited state where the optically induced lattice distortion is created (Nasu, 2003). In the relaxed excited state, a broad absorption band appears (Hasegawa & Tanaka, 2001; Okamura et al., 2006).

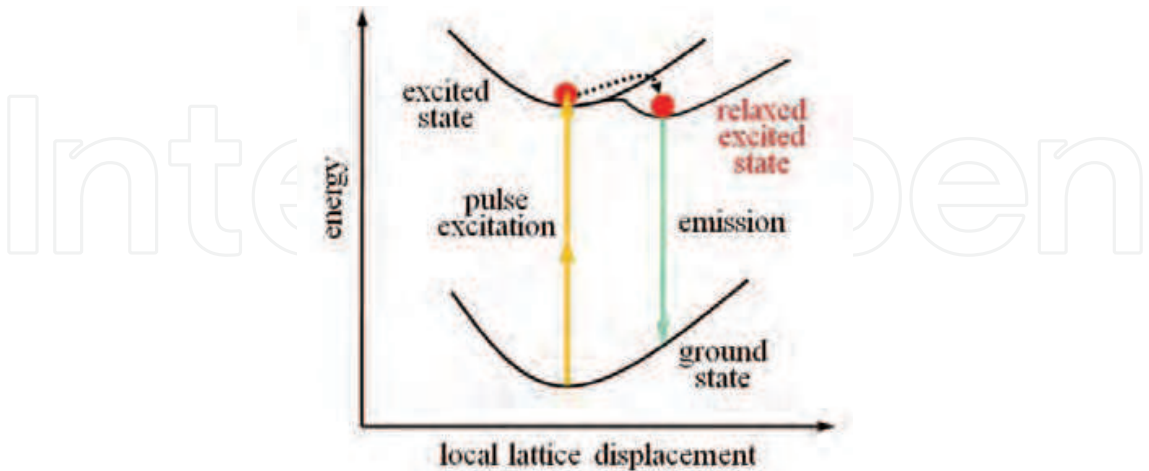


Fig. 11. Schematic diagram of the electronic states in SrTiO₃.

Figure 12 shows the emission spectra observed under two types of optical excitation; the pulse excitation of 790 nm and the UV illumination of 380 nm. As is seen, the two spectra are almost the same as each other. This result indicates that the same relaxed excited state is generated by the pulse excitation through a multi-photon absorption process. We observed the dynamics of the optically induced lattice distortion in the relaxed excited state generated by ultrashort pump pulses. The transient absorption and birefringence after the optical pulse excitation, which is originated in the generation of the relaxed excited state, is studied by the pump-probe technique to investigate the dynamical properties of the optically induced lattice distortion.

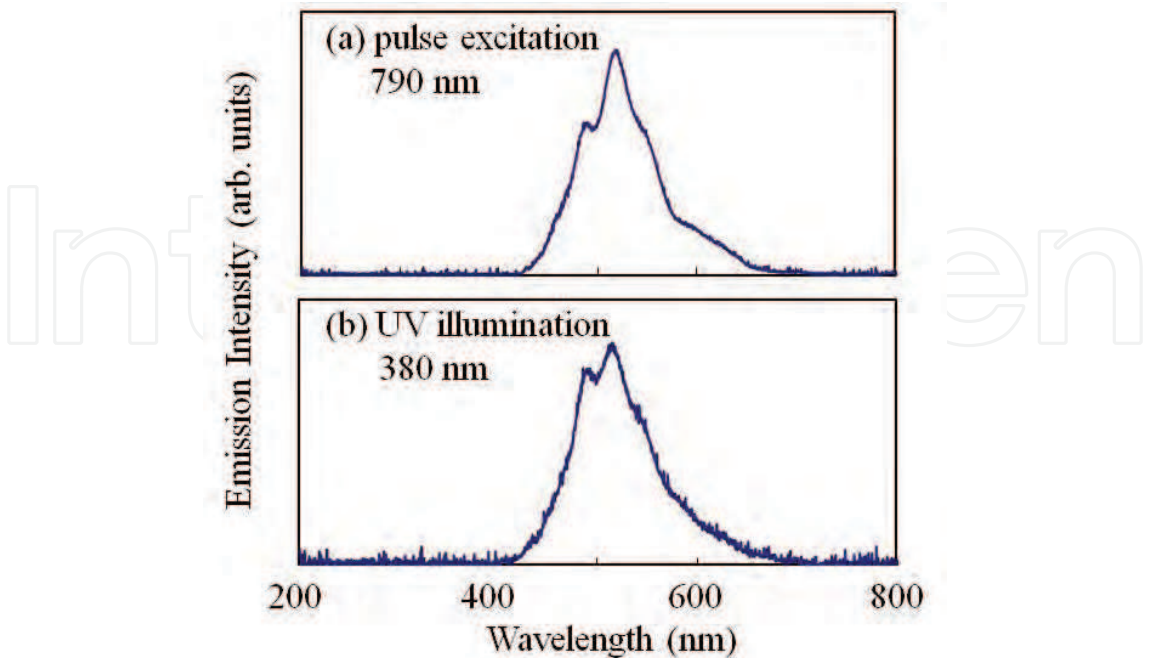


Fig. 12. Emission spectra observed (a) for the pulse excitation of 790 nm and (b) for the UV illumination of 380 nm.

4.1 Pump-probe measurement after the optical pulse excitation

The dynamics of the optically induced lattice distortion was observed by transient absorption and birefringence with the pump-probe technique. The lattice distortion is generated in the relaxed excited state by a linearly polarized pump pulse through a multi-photon absorption process. Induced time-dependent absorption or anisotropy of refractive index after the pulse excitation is detected as the change of the transmission or polarization of a linearly polarized probe pulse. The time evolution of the signal was observed by changing the optical delay between the pump and probe pulse.

The pump pulse is provided by a Ti:sapphire regenerative amplifier whose wavelength, pulse energy, and pulse width at the sample are 790 nm, 2 μ J, and 0.2 ps, respectively. In the experiment in the picosecond region, the probe pulse is provided by an optical parametric amplifier whose wavelength, pulse energy, and pulse width are 700 nm, 0.1 μ J, and 0.2 ps, respectively. The repetition rate of the pulses is 1 kHz. The time evolution of the signal is observed by changing the optical delay between the pump and probe pulses. The pump pulse is switched on and off shot by shot by using a photoelastic modulator, a quarter-wave plate, and a polarizer, and the output from the polarimeter is lock-in detected to improve the signal-to-noise ratio. In the experiment in the millisecond region, a continuous-wave probe light provided by a laser diode, whose wavelength is 660 nm, is used. The linearly polarized pump and probe beams are nearly collinear and perpendicular to the (001) surface of the sample, and are focused on the sample in a temperature-controlled refrigerator.

The transmission intensity is detected by a photodiode. The induced anisotropy of refractive index is detected by the polarimeter with a quarter-wave plate as the polarization change of the probe pulse. The plane of polarization of the probe pulse is tilted by 45° from that of the pump pulse. The two different wavelengths for the pump and probe lights and pump-cut filters are used to eliminate the leak of the pump light from the input of the photodiode or polarimeter.

4.2 Transient absorption in the picosecond region

It is found that the transmission is decreased after the optical pulse excitation. The transient absorption signal in SrTiO₃ have the component rising in the picosecond region as shown in Fig. 13. This rise time, which is of the order of 100 ps, corresponds to the generation time of the relaxed excited state.

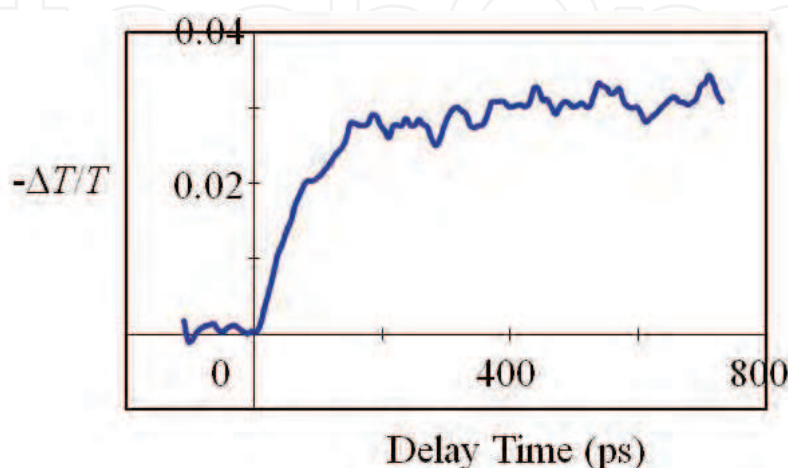


Fig. 13. Transient absorption signal in the picosecond region in SrTiO₃ at 6 K.

4.3 Transient absorption in the millisecond region

The temperature dependence of the transient absorption in the millisecond region in SrTiO_3 is shown in Fig. 14. The transient absorption signals have the decay time in the millisecond region. As the temperature is decreased, the signal amplitude is increased. The averaged occupation probability in the relaxed excited state strongly depends on the temperature and is large at low temperatures, where the photo-induced giant dielectricity is observed.

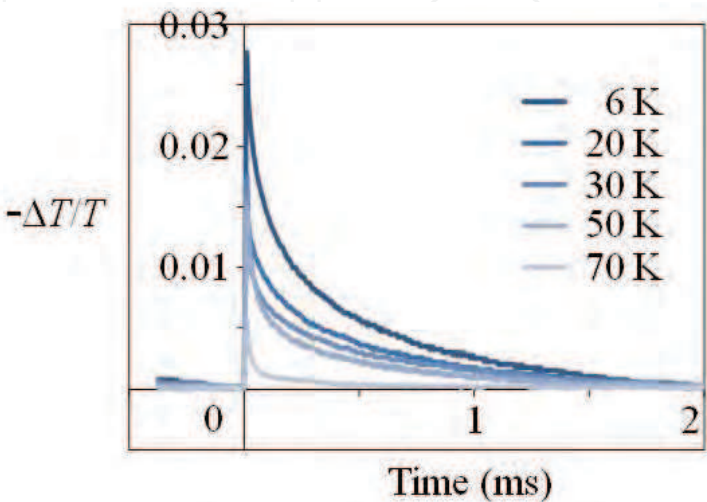


Fig. 14. Temperature dependence of the transient absorption in the millisecond region in SrTiO_3 .

4.4 Transient birefringence in the millisecond region

The time evolution of the lattice distortion is observed by transient birefringence measurement with the pump-probe technique. The temperature dependence of the transient birefringence in the millisecond region in SrTiO_3 is shown in Fig. 15. The observed signal curves of the transient birefringence and their temperature dependence show similar behavior to those of the transient absorption.

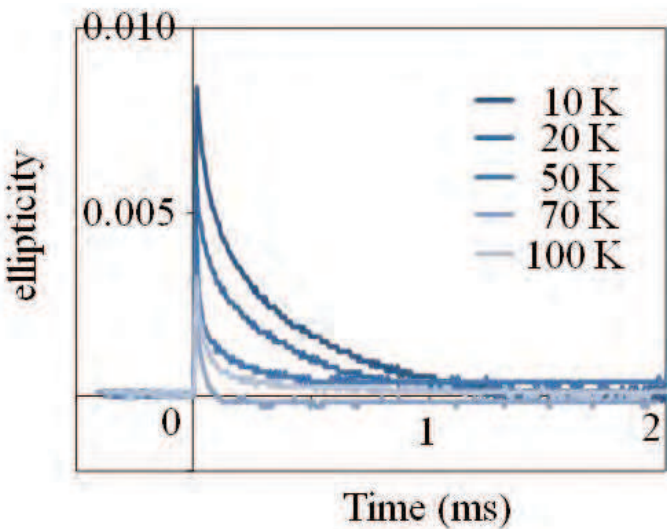


Fig. 15. Temperature dependence of the transient birefringence in the millisecond region in SrTiO_3 .

The photo-induced conductivity in SrTiO_3 , where the resistivity drops rapidly at low temperatures, has also been reported (Katsu et al., 2000). The photo-induced lattice distortion, absorption, and conductivity can be interpreted to have the same origin in the relaxed excited state. The experimental results suggest that the photo-induced effect in SrTiO_3 is consistent with the conductive-region model.

Giant dielectric response in nonferroelectric materials has been reported for grains surrounded by the insulating grain boundary and is explained by the Maxwell-Wagner model, namely the conductive-region model (Homes et al., 2001; Wu et al., 2002; Dwivedi et al., 2010). SrTiO_3 crystal is a stoichiometric material and has no grain structure. It may have a superposition of insulative and conductive regions under the UV illumination at low temperatures, whose structure may be related to the quantum paraelectricity under the dark illumination. However, the detail of the microscopic structure is unknown at present.

5. Conclusion

We observed the temperature dependences of the stationary birefringence, the transient birefringence in the pulsed electric field, and the transient absorption and birefringence after the optical pulse excitation to investigate the photo-induced effect in pure and Ca-doped SrTiO_3 .

The first-order-like structural deformation is found in the UV intensity dependence in Ca-doped SrTiO_3 , which begins at a very weak UV intensity of 10^{-3} mW/mm^2 . The generated lattice distortion is along the [100] axis as in the case of pure SrTiO_3 . The shift of the ferroelectric phase transition temperature toward the lower temperature side is observed under the UV illumination.

From the temperature dependence of the change in birefringence in Ca-doped SrTiO_3 in the four types of fields, where a UV light field is on or off and a DC electric field is on or off, it is found that a structural deformation is generated along the [100] axis under the UV illumination and its magnitude is of the same order as that of the ferroelectric deformation along the [110] axis.

It is found that the photo-induced lattice distortion is not affected by the electric field. The photo-induced lattice distortion, absorption, and conductivity are generated in the relaxed excited state, whose lifetime is in the millisecond region. These facts suggest that the photo-induced giant electric field in SrTiO_3 is consistent with the conductive-region model rather than the ferroelectric cluster model.

SrTiO_3 is a very peculiar material in which the dielectricity of the Maxwell-Wagner type appears in a stoichiometric material only under UV illumination at low temperatures. The origin of the enormous dielectric constants under UV illumination is considered to be different from that under dark illumination, although the latter is still not made clear.

6. Acknowledgement

We would like to thank Dr. Y. Yamada and Prof. K. Tanaka for providing us the samples of Ca-doped SrTiO_3 .

7. References

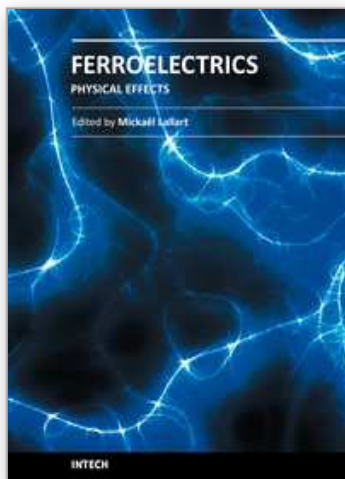
Bednorz, J. G. & Muller, K. A. (1984). $\text{Sr}_{1-x}\text{Ca}_x\text{TiO}_3$: An XY quantum ferroelectric with transition to randomness, *Phys. Rev. Lett.* Vol. 52, No. 25, (1984), pp. 2289-2292.

- Bianchi, U.; Kleeman, W. & Bednorz, J. G. (1994). Raman scattering of ferroelectric $\text{Sr}_{1-x}\text{Ca}_x\text{TiO}_3$, $x=0.007$, *J. Phys. Condens. Matter*, Vol. 6, No. 6, (1994), pp. 1229-1238.
- Dwivedi, G. D.; Tseng, K. F.; Chan, C. L.; Shahi, P.; Lourembam, J.; Chatterjee, B.; Ghosh, A. K.; Yang, H. D. & Chatterjee, S. (2010). Signature of ferroelectricity in magnetically ordered Mo-doped CoFe_2O_4 , *Phys. Rev. B*, Vol. 82, No. 13, (2010), 134428 (5 pages).
- Godefroy, G.; Jullien, P. & Cai, L. (1976). Photoconduction in doped BaTiO_3 single crystals, *Ferroelectrics*, Vol. 13, No. 1, (1976), pp. 309-312.
- Hasegawa, T.; Mouri, S.; Yamada, Y. & Tanaka, K. (2003). Giant photo-induced dielectricity in SrTiO_3 , *J. Phys. Soc. Jpn.*, Vol. 72, No. 1, (2003), pp. 41-44.
- Hasegawa, T. & Tanaka, K. (2001). Photo-induced polaron states in strontium titanate, *J. Lumin.*, Vol. 94-95, (2001), pp. 15-18.
- Homes, C. C.; Vogt, T.; Shapiro, S. M.; Wakimoto, S. & Ramirez, A. P. (2001). Optical response of high-dielectric-constant perovskite-related oxide, *Science*, Vol. 293, (2001), pp. 673-676.
- Jones, R. V. (1976). Rotary 'aether drag', *Proc. R. Soc. London, Ser. A*, Vol. 349, (1976), pp. 423-439.
- Katayama, I.; Ichikawa, Y. & Tanaka, K. (2003). Critical behaviors of photoinduced giant permittivity in potassium tantalate, *Phys. Rev. B*, Vol. 67, No. 10, (2003), 100102(R) (4 pages).
- Katsu, H.; Tanaka, H. & Kawai, T. (2000). Anomalous Photoconductivity in SrTiO_3 , *Jpn. J. Appl. Phys.* Vol. 39, (2000), pp. 2657-2658.
- Kohmoto, T.; Fukuda, Y.; Kunitomo, M. & Isoda, K. (2000). Observation of ultrafast spin-lattice relaxation in Tm^{2+} -doped CaF_2 and SrF_2 crystals by optical means, *Phys. Rev. B*, Vol. 62, No. 1, (2000), pp. 579-583.
- Koyama, Y.; Moriyasu, T.; Okamura, H.; Yamada, Y.; Tanaka, K. & Kohmoto, T. (2010). Doping-induced ferroelectric phase transition in strontium titanate: Observation of the birefringence and the coherent phonons under the ultraviolet illumination, *Phys. Rev. B*, Vol. 81, No. 2, (2010), 024104 (6 pages).
- Muller, K. A. & Burkard, H. (1979). SrTiO_3 : An intrinsic quantum paraelectric below 4 K, *Phys. Rev. B*, Vol. 19, No. 7, (1979), pp. 3593-3602.
- Nasu, K. (2003). Photogeneration of superparaelectric large polarons in dielectrics with soft anharmonic T_{1u} phonons, *Phys. Rev. B*, Vol. 67, No. 17 (2003), 174111 (8 pages).
- Okamura, H.; Matsubara, M.; Tanaka, K.; Fukui, K.; Terakami, M.; Nakagawa, H.; Ikemoto, Y.; Moriwaki, T.; Kimura, H. & Nanba, T. (2006). Photogenerated carriers in SrTiO_3 probed by mid-infrared absorption, *J. Phys. Soc. Jpn.*, Vol. 75, No. 2, (2006), 023703 (5 pages).
- Takesada, M.; Yagi, T.; Itoh, M. & Koshihara, S. (2003). A gigantic photoinduced dielectric constant of quantum paraelectric perovskite oxides observed under a weak DC electric field, *J. Phys. Soc. Jpn.*, Vol. 72, No. 1, (2003), pp. 37-40.
- Ueda, S.; Tatsuzaki, I. & Shindo, Y. (1967). Change in the dielectric constant of SbSI caused by illumination, *Phys. Rev. Lett.*, Vol. 18, No. 12, (1967), pp. 453-454.
- Volk, T. R.; Grekov, A. A.; Kosonogov, N. A. & Fridkin, V. M. (1973). Influence of illumination on the domain structure and the Curie temperature of BaTiO_3 , *Sov. Phys. Solid State*, Vol. 14, No. 11, (1973), pp. 2740-2743.
- Vugmeister, B. E. & Glinchuk, M. P. (1990). Dipole glass and ferroelectricity in random-site electric dipole systems, *Rev. Mod. Phys.*, Vol. 62, (1990), pp. 993-1026.

- Wu, J.; Nan, C. W.; Lin, Y. & Deng, Y. (2002). Giant dielectric permittivity observed in Li and Ti doped NiO, *Phys. Rev. Lett.*, Vol. 89, No. 21, (2002), 217601 (4 pages).
- Yamada, Y. & Tanaka, K. (2008). Mechanism of photoinduced dielectric response in ferroelectric $\text{Sr}_{1-x}\text{Ca}_x\text{TiO}_3$, *J. Phys. Soc. Jpn.* Vol. 77, No. 5, (2008), 54704 (10 pages).

IntechOpen

IntechOpen



Ferroelectrics - Physical Effects

Edited by Dr. Mickaël Lallart

ISBN 978-953-307-453-5

Hard cover, 654 pages

Publisher InTech

Published online 23, August, 2011

Published in print edition August, 2011

Ferroelectric materials have been and still are widely used in many applications, that have moved from sonar towards breakthrough technologies such as memories or optical devices. This book is a part of a four volume collection (covering material aspects, physical effects, characterization and modeling, and applications) and focuses on the underlying mechanisms of ferroelectric materials, including general ferroelectric effect, piezoelectricity, optical properties, and multiferroic and magnetoelectric devices. The aim of this book is to provide an up-to-date review of recent scientific findings and recent advances in the field of ferroelectric systems, allowing a deep understanding of the physical aspect of ferroelectricity.

How to reference

In order to correctly reference this scholarly work, feel free to copy and paste the following:

Toshiro Kohmoto and Yuka Koyama (2011). Photo-induced Effect in Quantum Paraelectric Materials Studied by Transient Birefringence Measurement, *Ferroelectrics - Physical Effects*, Dr. Mickaël Lallart (Ed.), ISBN: 978-953-307-453-5, InTech, Available from: <http://www.intechopen.com/books/ferroelectrics-physical-effects/photo-induced-effect-in-quantum-paraelectric-materials-studied-by-transient-birefringence-measuremen>

INTECH
open science | open minds

InTech Europe

University Campus STeP Ri
Slavka Krautzeka 83/A
51000 Rijeka, Croatia
Phone: +385 (51) 770 447
Fax: +385 (51) 686 166
www.intechopen.com

InTech China

Unit 405, Office Block, Hotel Equatorial Shanghai
No.65, Yan An Road (West), Shanghai, 200040, China
中国上海市延安西路65号上海国际贵都大饭店办公楼405单元
Phone: +86-21-62489820
Fax: +86-21-62489821

© 2011 The Author(s). Licensee IntechOpen. This chapter is distributed under the terms of the [Creative Commons Attribution-NonCommercial-ShareAlike-3.0 License](https://creativecommons.org/licenses/by-nc-sa/3.0/), which permits use, distribution and reproduction for non-commercial purposes, provided the original is properly cited and derivative works building on this content are distributed under the same license.

IntechOpen

IntechOpen